Signatures of shape phase transitions in odd-mass nuclei

Nomura, Kosuke; Nikšić, Tamara; Vretenar, Dario

Repository / Repozitorij:

Repository of the Faculty of Science - University of Zagreb

Signatures of shape phase transitions in odd-mass nuclei

K. Nomura,[1,2] T. Nikšić,[1] and D. Vretenar[1]

[1]*Physics Department, Faculty of Science, University of Zagreb, 10000 Zagreb, Croatia*
[2]*Center for Computational Sciences, University of Tsukuba, Tsukuba 305-8577, Japan*

Quantum phase transitions between competing ground-state shapes of atomic nuclei with an odd number of protons or neutrons are investigated in a microscopic framework based on nuclear energy density functional theory and the particle-plus-boson-core coupling scheme. The boson-core Hamiltonian, as well as the single-particle energies and occupation probabilities of the unpaired nucleon, are completely determined by constrained self-consistent mean-field calculations for a specific choice of the energy density functional and paring interaction, and only the strength parameters of the particle-core coupling are adjusted to reproduce selected spectroscopic properties of the odd-mass system. We apply this method to odd-A Eu and Sm isotopes with neutron number $N \approx 90$, and explore the influence of the single unpaired fermion on the occurrence of a shape phase transition. Collective wave functions of low-energy states are used to compute quantities that can be related to quantum order parameters: deformations, excitation energies, $E2$ transition rates, and separation energies, and their evolution with the control parameter (neutron number) is analyzed.

I. INTRODUCTION

Quantum phase transitions (QPTs) are a prominent feature of many-body systems in many fields of physics and chemistry [1]. Nuclear QPTs [2] are transitions between competing ground-state shapes (spherical, axially deformed shapes that are soft with respect to triaxial deformations) induced by variation of a nonthermal control parameter at zero temperature. Gradual transitions between different shapes in chains of isotopes or isotones predominate, but in a number of cases, with the addition or subtraction of only few nucleons, abrupt changes in ground-state properties are observed and related critical phenomena emerge [3,4]. When considering QPT in finite systems such as atomic nuclei, in particular, an essential question is how to identify observables that can be related to order parameters. In addition, discontinuities at a phase transitional point are smoothed out in finite nuclei, and it is not always possible to associate the point of phase transition with a particular nucleus, because the control parameter of shape phase transitions, that is, the nucleon number, is not continuous. Numerous experimental studies of transitional nuclei have been carried out in the last fifteen years, and signatures of first- and second-order QPTs have been identified and investigated with various theoretical methods (for a review see Ref. [2] and references cited therein). New and very active areas of research include excited-state quantum phase transitions [5–8] and QPTs in odd-mass nuclei [5,9,10].

QPTs between equilibrium shapes of even-even nuclei, that is, systems with both proton and neutron numbers (Z and N) even, have been extensively explored using a variety of phenomenological [2] and microscopic [11–14] approaches. A description of possible QPTs in odd-mass nuclei, in which either Z or N is an odd number, is considerably more complex. Because of the effect of pairing, in even-even systems all nucleons are coupled pairwise to $T = 1$ pairs, and the low-energy excitation spectra are characterised by collective vibrational and rotational degrees of freedom [3]. For odd-A nuclei both single-particle [unpaired fermion(s)] and collective

(even-even core) degrees of freedom determine the low-energy excitations [15]. Important issues when considering QPTs in odd-mass nuclei are the influence of the unpaired fermion(s) on the location and nature of the phase transition, empirical signatures of QPTs in odd-A nuclei, and the definition and computation of order parameters [9,10]. To address these questions, shape phase transitions in odd-mass systems have mainly been investigated using empirical approaches such as algebraic methods [9,10,16,17], and geometrical models [18,19]. Microscopic studies of QPTs in odd-mass nuclei, and in particular studies of quantum order parameters, have not been as extensively pursued as in the case of even-even systems.

This work presents a microscopic study of nuclear shape phase transitions in odd-mass systems in the rare-earth region with $N \approx 90$ and, in particular, an analysis of observables that can be related to order parameters. Recently we have developed a new theoretical method [20] based on nuclear density functional theory [21–23] and the particle-core coupling scheme [3,15]. The even-even core nucleus is modeled in terms of s and d boson degrees of freedom [24], which represent correlated pairs of valence nucleons, and the particle-core coupling of the unpaired proton or neutron is described in the framework of the interacting boson-fermion model (IBFM) [25]. In the model of Ref. [20] the parameters of the even-even boson-core Hamiltonian, and the single-particle energies and occupation probabilities of the odd-fermion states, are completely determined by a constrained self-consistent mean-field (SCMF) calculation for a specific choice of the energy density functional (EDF) and pairing interaction. Only the strength parameters of the fermion-boson coupling terms of the Hamiltonian are specifically adjusted to reproduce selected spectroscopic data for a given nucleus. The method has been illustrated and tested in an analysis of axially deformed odd-A nuclei $^{151–155}$Eu, and it has been shown that the approach enables a systematic, accurate, and computationally feasible description of low-energy spectroscopic properties of odd-mass nuclei [20].

In the present analysis we consider the structural evolution of odd-mass Eu ($Z = 63$) and Sm ($Z = 62$) isotopes in the region with neutron number $N \approx 90$. For the low-energy excitation spectra these systems can be treated as a single unpaired proton and neutron, respectively, coupled to the even-even core Sm nuclei. The boson-core nuclei, $^{146-154}$Sm, provide an outstanding example of a first-order QPT from spherical to axially deformed equilibrium shapes, with the control parameter being the neutron number [2,26]. The odd particle for the odd-A Sm nuclei is also a neutron, while that of the odd Eu isotopes is a proton, and this means a nucleon different from the control parameter of the boson core. We analyze the influence of the unpaired nucleon on the occurrence of a QPT in both cases.

Section II contains a concise outline of the theoretical method used in the present study. In Sec. III we analyze the theoretical low-energy positive- and negative-parity excitation spectra of odd-A Sm nuclei in comparison with available data, and explore signatures of spherical to axially deformed shape transitions in odd-mass Eu ($Z = 63$) and Sm ($Z = 62$): equilibrium deformation parameters, spectroscopic properties, and separation energies. Section IV includes a summary and a brief outlook for future studies.

II. MODEL FOR ODD-MASS NUCLEI

In Ref. [20] we introduced a novel method for calculating spectroscopic properties of medium-mass and heavy atomic nuclei with an odd number of nucleons, based on the framework of nuclear energy density functional theory and the particle-core coupling scheme. The model Hamiltonian $\hat{H}$ used to describe an odd-A nucleus contains a term that corresponds to the even-even boson-core $\hat{H}_B$ [built from monopole s (with spin and parity $J^\pi = 0^+$) and quadrupole d ($J^\pi = 2^+$) bosons], a single-particle Hamiltonian $\hat{H}_F$ that describes the unpaired nucleon(s), and an interaction term $\hat{H}_{BF}$ that couples the boson and fermion degrees of freedom:

$$\hat{H} = \hat{H}_B + \hat{H}_F + \hat{H}_{BF}. \tag{1}$$

The number of bosons N_B and the number of odd fermions N_F are conserved separately and, since we consider low-energy excitation spectra of odd-mass systems, $N_F = 1$. In the present version, therefore, the model space does not include three and higher (quasi)particle states. Since a boson represents a collective pair of valence nucleons, N_B corresponds to the number of fermion pairs, particle or hole, in the major valence shell [27]. In the present case N_B equals the number of fermion pairs outside the doubly magic nucleus ^{132}Sn, that is, from 7 to 11 for the boson-core nuclei $^{146-154}$Sm. We employ for the boson-core Hamiltonian the following form:

$$\hat{H}_B = \epsilon_d \hat{n}_d + \kappa \hat{Q}_B \cdot \hat{Q}_B + \kappa' \hat{L} \cdot \hat{L}, \tag{2}$$

with the d-boson number operator $\hat{n}_d = d^\dagger \cdot \tilde{d}$, the quadrupole operator $\hat{Q}_B = s^\dagger \tilde{d} + d^\dagger \tilde{s} + \chi [d^\dagger \times \tilde{d}]^{(2)}$, and the angular momentum operator $\hat{L} = \sqrt{10}[d^\dagger \times \tilde{d}]^{(1)}$. ϵ_d, κ, κ', and χ are parameters. The fermion Hamiltonian for a single nucleon reads $\hat{H}_F = \sum_j \epsilon_j [a_j^\dagger \times \tilde{a}_j]^{(0)}$, with ϵ_j the single-particle energy of the spherical orbital j. For the particle-core coupling

$\hat{H}_{BF}$ we use the simplest form [25,28]:

$$\hat{H}_{BF} = \sum_{jj'} \Gamma_{jj'} \hat{Q}_B \cdot [a_j^\dagger \times \tilde{a}_{j'}]^{(2)} + \sum_{jj'j''} \Lambda_{jj'}^{j''} : [[d^\dagger \times \tilde{a}_j]^{(j'')}$$
$$\times [a_{j'}^\dagger \times \tilde{d}]^{(j'')}]^{(0)} : + \sum_j A_j [a^\dagger \times \tilde{a}_j]^{(0)} \hat{n}_d, \tag{3}$$

where the first, second, and third terms are referred to as the quadrupole dynamical, exchange, and monopole interactions, respectively. The strength parameters $\Gamma_{jj'}$, $\Lambda_{jj'}^{j''}$, and A_j can be expressed, by use of the generalized seniority scheme, in the following j-dependent forms [29]:

$$\Gamma_{jj'} = \Gamma_0 \gamma_{jj'}, \tag{4}$$

$$\Lambda_{jj'}^{j''} = -2\Lambda_0 \sqrt{\frac{5}{2j''+1}} \beta_{jj'} \beta_{j'j''}, \tag{5}$$

$$A_j = -A_0 \sqrt{2j+1}, \tag{6}$$

where $\gamma_{jj'} = (u_j u_{j'} - v_j v_{j'}) Q_{jj'}$ and $\beta_{jj'} = (u_j v_{j'} + v_j u_{j'}) Q_{jj'}$, and the matrix element of the quadrupole operator in the single-particle basis $Q_{jj'} = \langle j || Y^{(2)} || j' \rangle$. The factors u_j and v_j denote the occupation probabilities of the orbit j, and satisfy $u_j^2 + v_j^2 = 1$. Γ_0, Λ_0, and A_0 denote the strength parameters. A more detailed discussion of each term of the Hamiltonian in Eq. (1) is included in Ref. [20].

To build the boson-fermion Hamiltonian in a first step one determines the parameters of the boson Hamiltonian $\hat{H}_B$, following the procedure introduced in Ref. [30]: the microscopic deformation energy surface, calculated with the constrained self-consistent mean-field (SCMF) method for a specific choice of the nuclear energy density functional (EDF) and a pairing interaction, is mapped onto the corresponding expectation value of the interacting boson Hamiltonian in the boson coherent state [31]. This procedure uniquely determines the parameters in the boson Hamiltonian $\hat{H}_B$.

The fermion model space contains all the spherical major shell valence orbitals of the unpaired particle, proton or neutron. In the present calculation we include spherical single-particle orbitals in the proton major shell $Z = 50-82$ (positive parity $1g_{7/2}, 2d_{5/2}, 2d_{3/2}, 3s_{1/2}$ and negative parity $1h_{11/2}$) for the odd-Z Eu isotopes, and the orbitals in the neutron major shell $N = 82-126$ (positive parity $1i_{13/2}$ and negative parity $1h_{9/2}, 2f_{7/2}, 2f_{5/2}, 3p_{3/2}, 3p_{1/2}$) for the odd-$N$ Sm nuclei. The canonical single-particle energies and occupation probabilities of these orbitals determine the terms $\hat{H}_F$ and $\hat{H}_{BF}$ of the Hamiltonian, respectively, and are obtained from the SCMF calculation constrained to zero deformation.

In the final step the strength parameters of the boson-fermion Hamiltonian $\hat{H}_{BF}$ are adjusted for each nucleus separately. Optimal values of the corresponding strength parameters (Γ_0, Λ_0, and A_0) are adjusted to reproduce the ground-state spin and/or the excitation energies of a few lowest levels, separately for positive- and negative-parity states.

The resulting Hamiltonian of Eq. (1) is diagonalized numerically [32] in the spherical basis $|j, L, \alpha, J\rangle$, where α is a generic notation for a set of quantum numbers n_d, ν, n_Δ that distinguish states with the same boson angular

momentum L [24], and J is the total angular momentum of the Bose-Fermi system ($|L - j| \leqslant J \leqslant L + j$). Using the wave functions resulting from the diagonalization, electromagnetic transition rates can be calculated. The relevant decay mode in the present study is the electric quadrupole ($E2$) transition. The $E2$ transition operator of the Bose-Fermi system reads $\hat{T}^{(E2)} = e_B \hat{Q}_B + e_F \hat{Q}_F$, where $\hat{Q}_B$ and $\hat{Q}_F$ are the quadrupole operators for the boson and fermion systems [20], respectively, and e_B and e_F are the effective charges. e_B is adjusted to reproduce the experimental $B(E2; 2^+_1 \rightarrow 0^+_1)$ value for the boson-core nucleus, while the constant value $e_F = 1.0$ eb is used for the fermion effective charge.

III. QUANTUM SHAPE PHASE TRANSITIONS IN ODD-MASS Sm AND Eu ISOTOPES

Probably the best example of a QPT in atomic nuclei is in the rare earth region with $N \approx 90$ neutrons, where a transition between spherical and axially symmetric equilibrium shapes has been extensively investigated both experimentally [33–39] and by using a number of theoretical methods [11,26,40–44]. Sm nuclei in this mass region, and ^{152}Sm in particular, was the first reported empirical example of a structure at the critical point of a first-order transition between a vibrator and the axial rotor phase [40]. Here we analyze low-energy states of odd-proton Eu nuclei and odd-neutron Sm nuclei that can be described by coupling the corresponding unpaired nucleon to the even-even Sm boson core.

The deformation energy surfaces for a set of even-even Sm core nuclei, which determine the parameters of the interacting-boson Hamiltonian, are calculated as functions of the polar deformation parameters β and γ, using the the constrained self-consistent relativistic Hartree-Bogoliubov (RHB) model, based on the energy density functional DD-PC1 [45], and a separable pairing force of finite range [46]. The map of the energy surface as a function of quadrupole deformation is obtained by imposing constraints on the axial and triaxial mass quadrupole moments. In Fig. 1 we display the self-consistent RHB triaxial quadrupole binding energy maps of the even-even $^{148-154}$Sm in the β-γ plane ($0 \leqslant \gamma \leqslant 60°$). The energy maps clearly exhibit a gradual increase of deformation of the prolate minimum with increasing neutron number, from spherical ^{146,148}Sm to well-deformed prolate shapes at and beyond ^{154}Sm, and the evolution of the γ dependence of the potentials. The axial potential barrier at zero deformation increases with mass number. With increasing N the prolate deformation of Sm isotopes at equilibrium becomes more pronounced and the shape evolution corresponds, in the language of the interacting boson model, to a transition between the U(5) and SU(3) limits of the Casten symmetry triangle [28]. The energy surfaces of ^{150,152}Sm indicate that these are transitional nuclei, characterized by a softer potential around the equilibrium minimum both in the β and γ directions. The softness of the energy surface with respect to the quadrupole deformation parameters β and/or γ around the mean-field equilibrium minimum has been associated with the phenomenon of quantum shape phase transition [2].

A phase transition is characterized by a significant variation of one or more order parameters as functions of the control
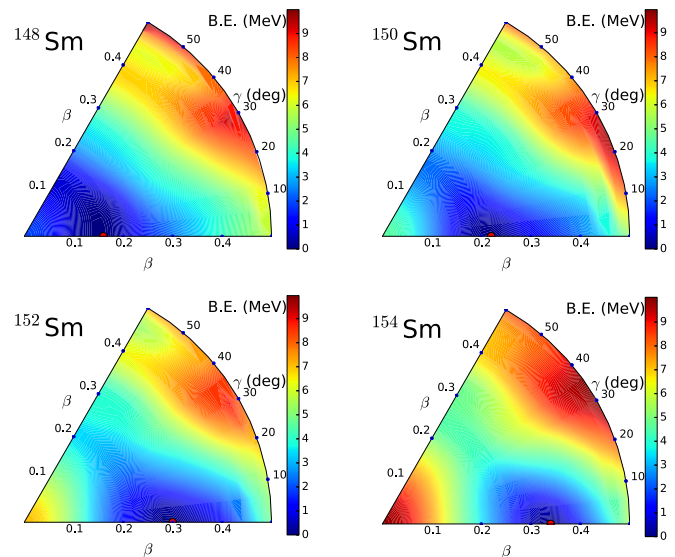

FIG. 1. Self-consistent RHB triaxial quadrupole binding energy maps of the even-even $^{148-154}$Sm isotopes in the β-γ plane ($0 \leqslant \gamma \leqslant 60°$). For each nucleus the energy surface is normalized with respect to the binding energy of the absolute minimum.

parameter. Even though shape phase transitions in nuclei have been explored extensively by considering potential energy surfaces, the deformation parameters that characterize these surfaces are not observables and, therefore, a quantitative study of QPT must go beyond the simple Landau approach and include the direct computation of observables related to order parameters. In the following we will consider spectroscopic properties of odd-mass Eu and Sm isotopes that can be associated with order parameters of a shape phase transition. To illustrate the capability of the present method to describe low-energy spectra of odd-mass nuclei in this region, in Figs. 2–5 we show results for the three lowest positive- and negative-parity bands of ^{149,151,153,155}Sm isotopes, in comparison with the available experimental values [47]. The calculated energy levels are grouped into bands according to the dominant $E2$ decay pattern. We note that the energy spectrum of ^{147}Sm is very similar to that of the adjacent nucleus ^{149}Sm, and available data are not sufficient for a detailed comparison. The calculated excitation spectra of odd-mass Eu nuclei have already been compared to data in Ref. [20], including $E2$ and $M1$ transition rates, spectroscopic quadrupole moments and magnetic moments, and this is why these spectra are not explicitly shown here.

For ^{149}Sm, in Fig. 2 one notices that both positive- and negative-parity bands exhibit a vibrational level structure characterized by the $\Delta J = 2$ systematics of the weak-coupling limit. The agreement between the calculated and experimental spectra is fairly good. The excitation spectrum of ^{151}Sm, shown in Fig. 3, is less harmonic and the levels are more compressed in energy. All bands, however, still display the $\Delta J = 2$ structure indicating that the odd neutron is not strongly coupled to the boson core.

A significant change in the structure of excitation spectra occurs between ^{151}Sm and ^{153}Sm (Fig. 4). Both in experiment
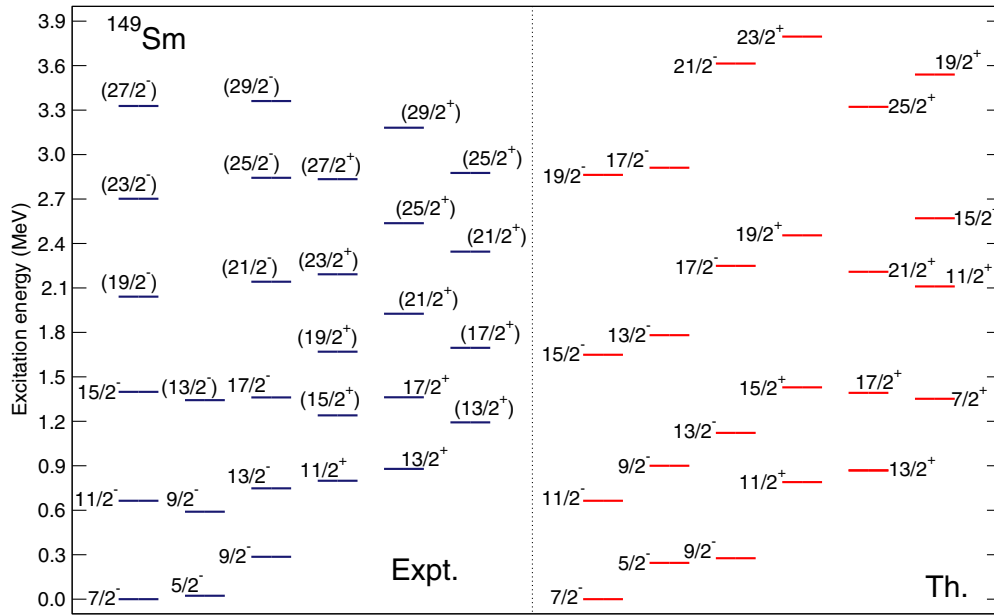
FIG. 2. The lowest three negative- and positive-parity bands of ^{149}Sm. Available data are compared to model calculation in which states are classified in bands according to dominant $E2$ transitions. The data are from Ref. [47], and parentheses denote states with only a tentative assignment of spin and parity.

and model calculations $\Delta J = 1$ bands characteristic for the strong-coupling limit are formed, and coexist with bands that exhibit the weak-coupling $\Delta J = 2$ systematics. In addition, ^{153}Sm is the only nucleus among all the odd-mass Sm isotopes considered in which the ground state has positive parity, originating from the neutron $1i_{13/2}$ orbit. The spectrum of ^{153}Sm reflects the abrupt change of structure at $N = 90$ in the even-even boson core, that can approximately be characterized by the X(5) analytic solution at the critical point of the first-order quantum phase transition between spherical and

axially deformed shapes [44]. We note that in experiment all the negative-parity bands display the strong-coupling structure, whereas both $\Delta J = 2$ and $\Delta J = 1$ sequences of negative-parity states are obtained in the model calculation. This discrepancy can most probably be attributed to the occupation probabilities of the corresponding single-particle orbitals obtained in the SCMF calculation. In addition, some structures could be based on intruder orbitals that develop from the shell below the neutron $N = 82$ closure and, therefore, beyond the model space in which the IBFM Hamiltonian is
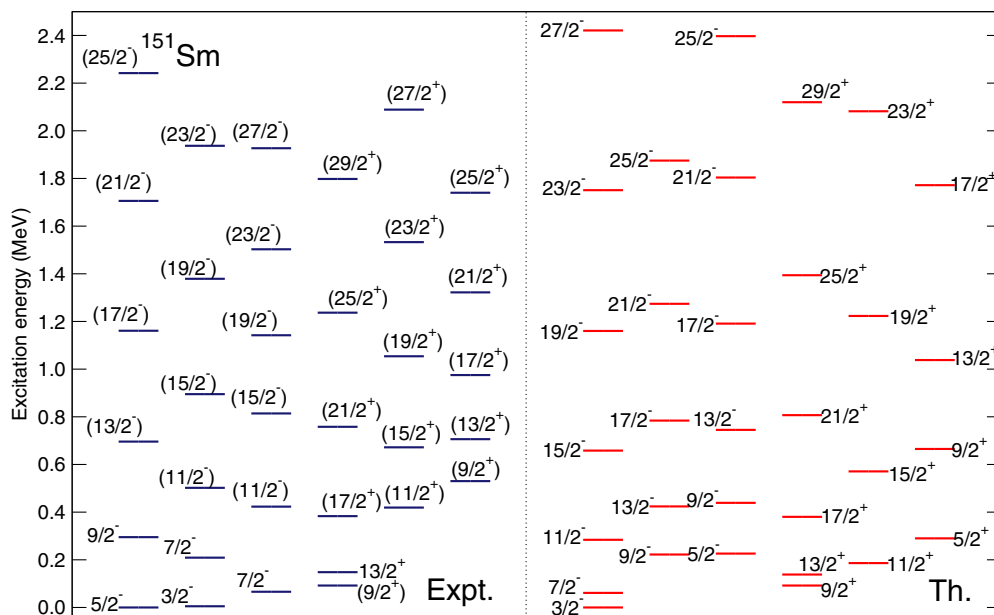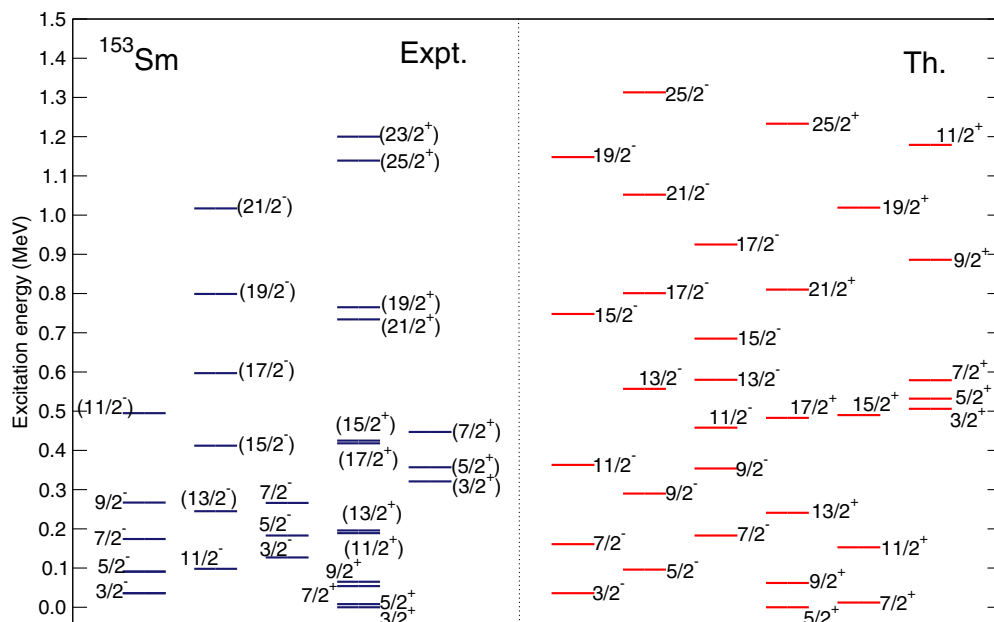

FIG. 3. Same as in the caption to Fig. 2, but for ^{151}Sm.

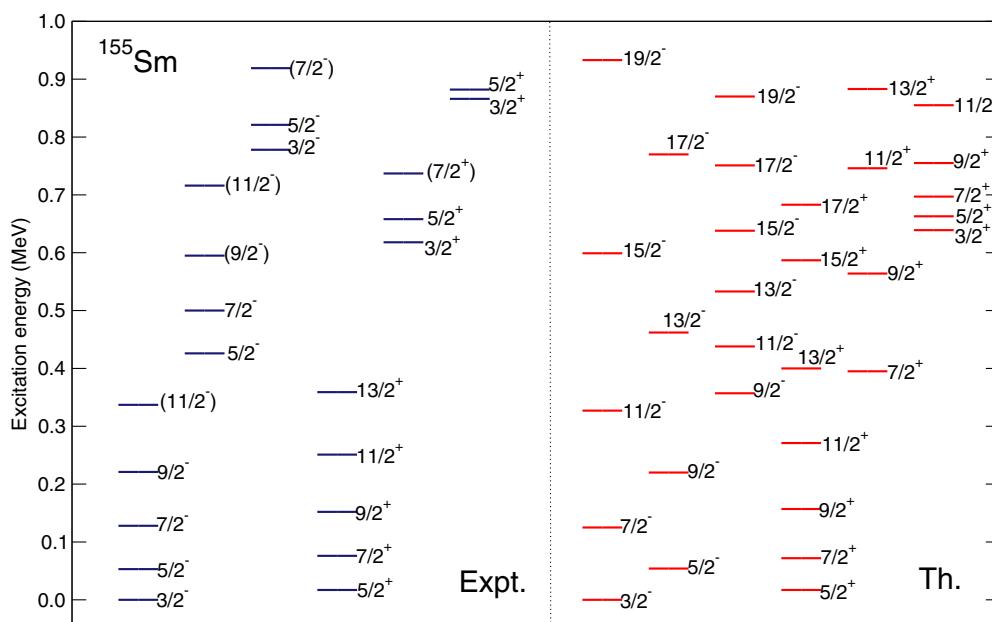FIG. 4. Same as in the caption to Fig. 2, but for ^{153}Sm.

diagonalised. For instance, the experimental band built on the state $11/2^-_1$ has been attributed to the neutron configuration $11/2^-[505]$ [47].

The transition to a well deformed, axially symmetric shape, is completed in ^{154}Sm (cf. Fig. 1), and this is clearly reflected in the excitation spectrum of ^{155}Sm, shown in Fig. 5. Sequences of both negative- and positive-parity states exhibit the $\Delta J = 1$ structure of the strong-coupling limit and the excitation energies follow to a good approximation the simple rotational $J(J + 1)$ pattern.

We note that, as already shown in our previous article of Ref. [20], a similar level of quantitative agreement with data

is obtained for the odd-mass Eu isotopes. The band structure of Eu nuclei is simpler than that of the corresponding odd Sm isotopes: in $^{147-151}$Eu the lowest three positive-parity bands follow the $\Delta J = 1$ systematics of the strong-coupling limit, while the lowest three negative-parity bands exhibit the weak-coupling $\Delta J = 2$ structure; in ^{153,155}Eu the lowest three bands of both positive- and negative-parity are characterized by the strong-coupling $\Delta J = 1$ sequence of states.

To analyze the overall systematics of excitation spectra in the transition from spherical to deformed equilibrium shapes, in Figs. 6 and 7 we plot the calculated spectra for the low-lying positive ($\pi = +1$) and negative parity ($\pi = -1$) yrast

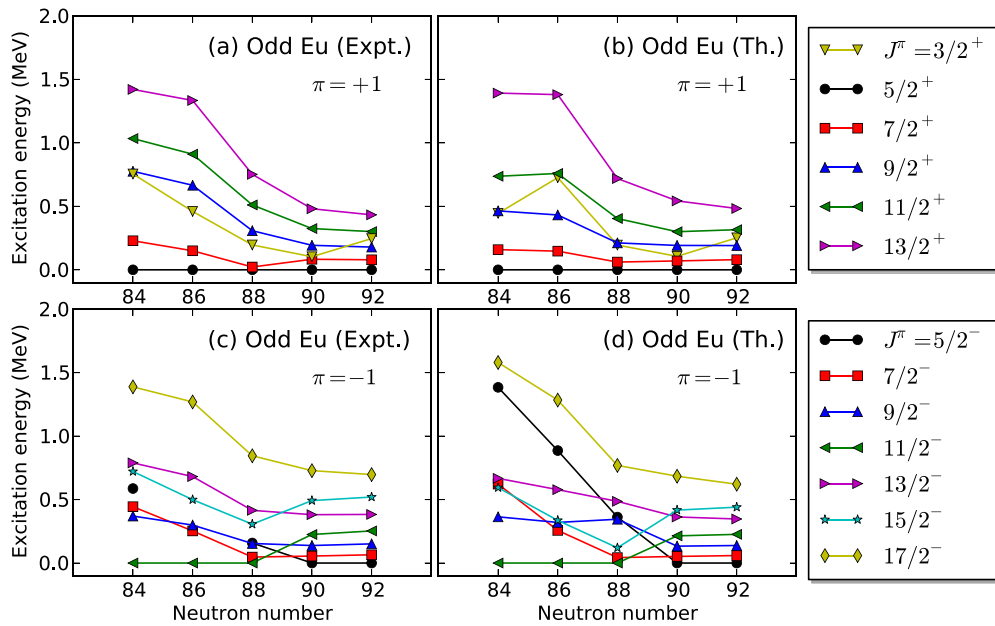FIG. 5. Same as in the caption to Fig. 2, but for ^{155}Sm.

FIG. 6. Evolution of excitation energies of low-lying [(a) and (b)] positive- ($\pi = +1$) and [(c) and (d)] negative-parity ($\pi = -1$) yrast states as functions of neutron number in the isotopes $^{147-155}$Eu, in comparison with available data taken from Ref. [47].

states in the isotopes $^{147-155}$Eu and $^{147-155}$Sm, as functions of neutron number, and compare them with available data [47]. For both odd-A Eu and Sm isotopes the model reproduces the experimental systematics, except for a few states in odd-A Sm isotopes with $N = 89$ or 91. The phase transition is characterized by a change in the spin of the ground state for a particular nucleus [10]. Indeed one notices that the ground-state spin changes at $N = 90$ in the Eu isotopes for negative parity, and at $N = 89$ in odd-A Sm for both parities. For the positive-parity states in Eu, however, the change does not occur and the $5/2^+$ level remains the ground state for all isotopes.

In the remainder of this section possible signatures of QPTs are explored in odd-mass Eu (odd proton) and Sm (odd neutron) nuclei at $N \approx 90$. We start by considering the equilibrium axial deformation parameter β which, even though it is not an observable, can nevertheless be used in a theoretical analysis to describe the evolution of deformation with the control parameter and as a signature of QPT in both even-even and odd-mass systems, as shown in the classical study of Ref. [9] using the IBFM. However, in contrast to a mean-field description of QPT based on the analysis of potential energy surfaces around equilibrium minima, we
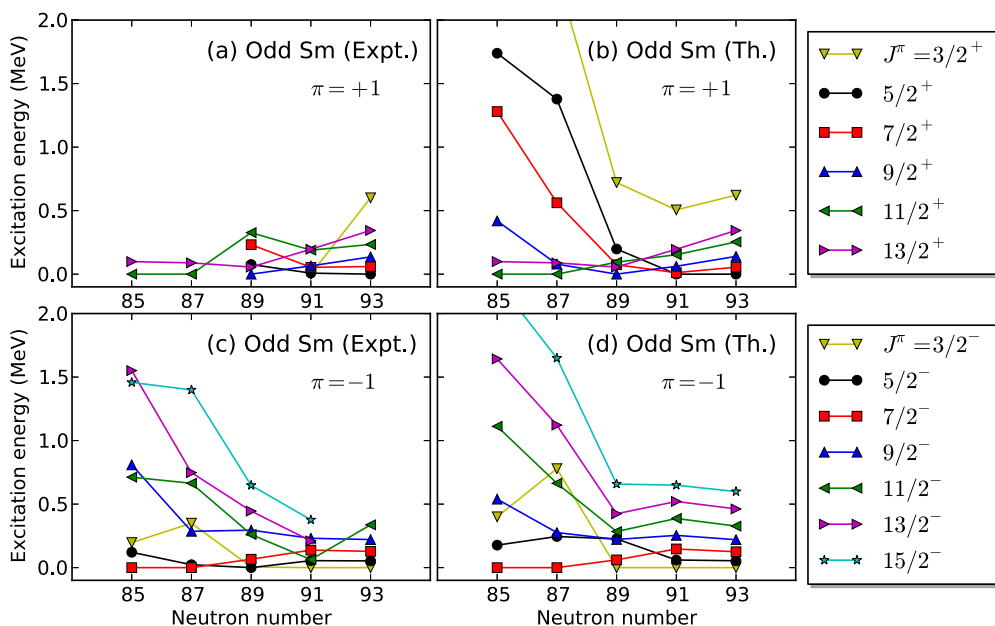

FIG. 7. Same as in the caption to Fig. 6, but for the isotopes $^{147-155}$Sm.
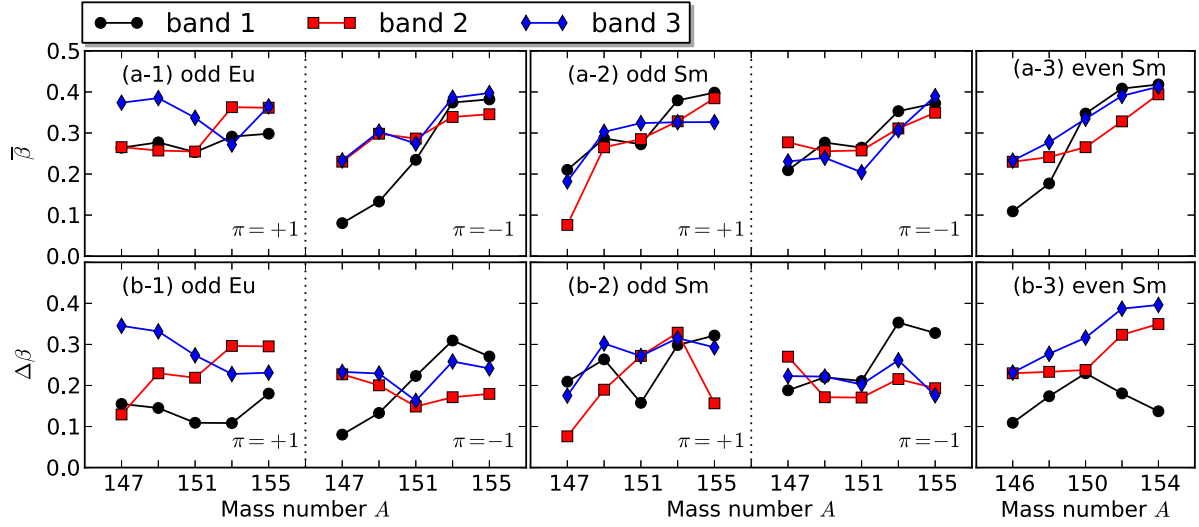
FIG. 8. Evolution of characteristic mean-field quantities calculated for the lowest three positive- ($\pi = +1$) and negative-parity ($\pi = -1$) bands of the odd-A Eu and Sm nuclei, and $K^\pi = 0^+$ bands in the even-A Sm isotopes, as functions of mass number: the mean value $\overline{\beta}$ (a) and variance $\Delta\beta$ (b) of the equilibrium deformation parameter for the bandhead state. "band 1," "band 2," and "band 3" denote the lowest, second-lowest, and third-lowest bands, respectively. See the main text for the definition of each quantity.

explicitly compute the deformation parameter for a given state using the wave function obtained by diagonalizing the IBFM Hamiltonian $\hat{H}$ in Eq. (1). Figure 8 displays the mean value of axial quadrupole deformation $\overline{\beta} = \sqrt{\langle \beta^2 \rangle}$ [panels (a-1), (a-2), (a-3)] and the variance $\Delta\beta = \sqrt{\langle \beta^2 \rangle - \langle \beta \rangle^2}$ [(b-1), (b-2), (b-3)] for the considered odd Eu and Sm isotopes, as well as the corresponding even-even Sm cores, calculated for the bandheads of three lowest positive ($\pi = +1$) and negative-parity ($\pi = -1$) bands. Note that for the even-even Sm nuclei all values included in Fig. 8 correspond to the lowest three $K^\pi = 0^+$ bands, where K^π denotes the projection of the total angular momentum on the symmetry axis of the intrinsic frame. The expectation value $\langle \beta^\lambda \rangle$ ($\lambda = 1,2$) for the state with spin and parity J^π, which is used in the calculation of $\overline{\beta}$ and $\Delta\beta$, is defined by the relation

$$\langle \beta^\lambda \rangle = \langle \Psi_{J,k} | \beta^\lambda | \Psi_{J,k} \rangle$$
$$= \int d\beta \langle \Psi_{J,k} | \phi_{J,k}(\beta) \rangle \beta^\lambda \langle \phi_{J,k}(\beta) | \Psi_{J,k} \rangle$$
$$= \int d\beta \beta^\lambda |\langle \phi_{J,k}(\beta) | \Psi_{J,k} \rangle|^2, \qquad (7)$$

where $|\Psi_{J,k}\rangle$ is the eigenstate of the IBFM Hamiltonian, with k distinguishing states with the same J, and $|\phi_{J,k}(\beta)\rangle$ is the projected intrinsic state of the coupled boson-fermion system [48,49]. In the integral of Eq. (7) the expectation value is computed in the interval $|\beta| < 0.6$. Values of β larger than 0.6 are not relevant because of the restricted boson model space built from a limited number of valence nucleon pairs. Consistent with the evolution of the equilibrium minimum at the mean-field level (cf. Fig. 1), the average deformation $\overline{\beta}$ in most cases increases monotonically with nucleon number to a value of approximately 0.35 for heavier isotopes. In the odd-mass Eu and Sm nuclei one notices a significant change from $A = 151$ to 153. Similarly, the variance $\Delta\beta$ changes (either increases or decreases) mostly for the transitional

nuclei with $A = 151$ or 153. The calculated values of $\overline{\beta}$ and $\Delta\beta$ evolve as expected; that is, the fluctuations in shape variables increase as a result of comparatively softer potentials in transitional nuclei.

The evolution of $E2$ transition rates with neutron number can also indicate a sudden change of deformation. In analogy to the quadrupole shape invariant q_2 which provides a measure of axial deformation in even-even nuclei [50,51], here we consider the quantity $\overline{B(E2)}$, defined as the average $B(E2)$ for transitions between the band-head of a given band with spin J_0 and the lowest n states with spin $J_0 + \Delta J$:

$$\overline{B(E2)} = \frac{1}{n} \sum_{k=1}^{n} B(E2; (J_0 + \Delta J)_k \to J_0), \qquad (8)$$

where $\Delta J = 1$ or 2, and the sum is in order of increasing excitation energies of the levels $J_0 + \Delta J$. Only a few lowest transitions will contribute significantly to this quantity and, therefore, $n = 5$ terms have been included in the sum. In the following the average $B(E2)$ transition defined in Eq. (8) is referred to as q invariant.

In the case of even-even nuclei quadrupole shape invariants have been used to quantify the first-order QPT between spherical and axially deformed shapes. In Ref. [43], based on the available data on deformed Gd isotopes and on a schematic IBM-1 calculation, the crossing of q invariants of the ground and first excited 0^+ states has been shown to occur near the point of shape phase transition. In Figs. 9(a) and 9(b) we plot the evolution of $\overline{B(E2)}$ for the ground (0_1^+) and first excited 0_2^+ states in the even-even Sm isotopes, and their difference as functions of mass number. Even though the present model calculation does not exhibit the crossing of the q invariants for 0_1^+ and 0_2^+, some basic features are still observed in Figs. 9(a) and 9(b): for the lighter isotopes the two q invariants are almost identical in magnitude and display a similar increase with mass number whereas, starting
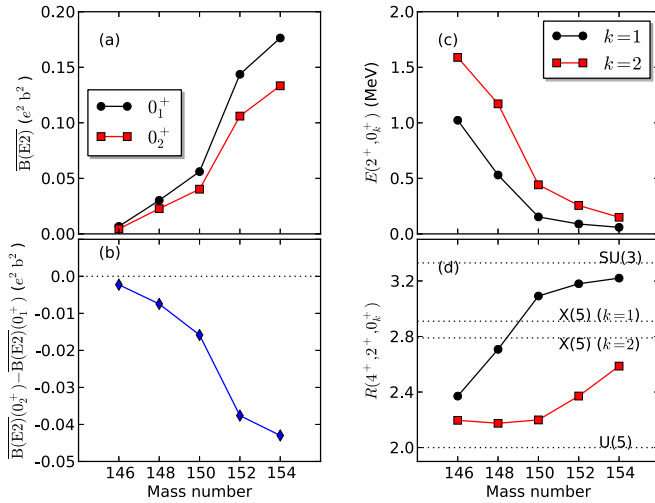
FIG. 9. Left: calculated values of $\overline{B(E2)}$ for the two lowest 0^+ states (a), and the difference $\overline{B(E2)}(0_2^+) - \overline{B(E2)}(0_1^+)$ (b) for the even-even Sm isotopes. Right: the excitation energies $E(2^+, 0_k^+)$ ($k = 1, 2$) of the states 2^+ (c) and the energy ratio of the 4^+ to the 2^+ excited states $R(4^+, 2^+, 0_k^+)$ (d) for the $K^\pi = 0_1^+$ and 0_2^+ bands of the even-even core nuclei $^{146-154}$Sm. In panel (d) the corresponding values of the energy ratio $E(4_1^+)/E(2_1^+)$ in the U(5), X(5), and SU(3) limits: 2.00, 2.91 ($k = 1$), 2.79 ($k = 2$), and 3.33, respectively, are also indicated by dotted lines.

from the point of phase transitions between ^{150}Sm and ^{150}Sm, their difference $\overline{B(E2)}(0_2^+) - \overline{B(E2)}(0_1^+)$ increases rapidly in magnitude and the q invariant (deformation) of the ground state becomes considerably larger.

To analyze how the odd particle influences the location and nature of the QPT observed in the even-even core, in Figs. 10(a)–10(d) we display the calculated values of the q invariant $\overline{B(E2)}$ of bandhead states for the three lowest positive- ($\pi = +1$) and negative-parity ($\pi = -1$) bands in the odd-A Eu and Sm isotopes, for the two cases of $\Delta J = 1$ and $\Delta J = 2$ transitions. In analogy to the even-even case shown in Figs. 9(a) and 9(b), one expects the q invariants to increase with neutron number. This feature does not seem to generally apply in the present calculation on the odd-A Eu and Sm nuclei; rather it depends on whether a band exhibits a weak-coupling or strong-coupling systematics. In the negative-parity bands of the odd-A Sm nuclei in Figs. 10(b) and 10(d), for instance, the q invariants of the bandhead states of the lowest and second-lowest bands do not display a notable change from $A = 151$ to 155 in the $\Delta J = 1$ case, whereas the q invariant of the bandhead state of the third-lowest band increases. In the $\Delta J = 2$ case the opposite is observed: the q invariants of the lowest and second-lowest bands increase with neutron number, whereas that of the third-lowest band remains almost unchanged. As shown in Figs. 4 and 5, the lowest two negative-parity bands of ^{153,155}Sm follow the $\Delta J = 2$ decay systematics typical of the weak-coupling limit, whereas the third-lowest negative-parity band follows the strong-coupling systematics and $E2$ transitions with $\Delta J = 1$ dominate. Nevertheless, one expects that the most significant change (either an increase or decrease) of the q invariants occurs between $A = 149$ and

151, or between $A = 151$ and 153, in accordance with the even-even case exhibiting an abrupt change of this quantity between $A = 150$ and 152.

Shape transitions can be also characterized by the evolution of excitation energies, as shown in Figs. 10(e) and 10(f) where we plot, for the three lowest bands of both parities, the energy difference

$$E(J_1, J_0) = E(J_1) - E(J_0). \tag{9}$$

$E(J_0)$ and $E(J_1)$ ($J_1 = J_0 + \Delta J$ with $\Delta J = 1, 2$) are the energies of the bandhead and the first excited state in a band, respectively. With the exception of an increase from mass $A = 147$ to 149 for two bands in odd-A Eu isotopes that can probably be attributed to a more pronounced band mixing, the quantity $E(J_1, J_0)$ decreases with neutron number, with a rapid change in the transitional nuclei at $N \approx 90$. Indeed, the 2^+ excitation energies in the bands $K^\pi = 0_1^+$ and 0_2^+ belonging to the corresponding even-even Sm nuclei and plotted in Fig. 9(c) exhibit a sudden decrease from $A = 148$ to 150 that reflects the abrupt rise of deformation. As another signature of the shape phase transition related to excitation energies, we consider the energy ratio between the lowest two excited states (with spin $J_1 = J_0 + \Delta J$ and $J_2 = J_0 + 2\Delta J$) in a given band:

$$R(J_2, J_1, J_0) = \frac{E(J_2) - E(J_0)}{E(J_1) - E(J_0)}. \tag{10}$$

In the even-even case this is nothing but the ratio of the 4^+ to 2^+ excitation energies in $K^\pi = 0^+$ bands and, especially the ratio in the yrast band, $R(4_1^+, 2_1^+, 0_1^+) = E(4_1^+)/E(2_1^+)$ has often been used as a signature of phase transition between vibrational and rotational nuclei. In Fig. 9(d) we plot the evolution of the ratio $R(4^+, 2^+, 0^+)$ for the lowest two bands with $K^\pi = 0^+$ in the even-A Sm isotopes as function of the mass (neutron) number. The ratio $R(4_1^+, 2_1^+, 0_1^+)$ exhibits a typical increase as a function of A, from close to the vibrational [or U(5)] limit [$R(4_1^+, 2_1^+, 0_1^+) = 2.00$], to the rotational [or SU(3)] limit [$R(4_1^+, 2_1^+, 0_1^+) = 3.33$]. The $R(4_1^+, 2_1^+, 0_1^+)$ value of 2.91, predicted by the X(5) critical-point symmetry model for the phase transition [26], is located between $A = 148$ and 150. The ratio $R(4^+, 2^+, 0_2^+)$ also exhibits an increase, but is always smaller than $R(4_1^+, 2_1^+, 0_1^+)$, and smaller than the value predicted by the X(5) model. The value of the ratio $R(4^+, 2^+, 0_2^+)$ differs from that of $R(4_1^+, 2_1^+, 0_1^+)$ particularly in the transitional nuclei, reflecting the different intrinsic structures of the two lowest 0^+ states. A similar trend is observed in the odd-A nuclei: Figs. 10(g) and 10(h) show the calculated values of the ratio $R(J_2, J_1, J_0)$ for the lowest three positive- and negative-parity bands in the considered odd-A Eu and Sm isotopes, respectively. In the vibrational ($A = 147$ and 149) and deformed rotational ($A = 153$ and 155) nuclei, the calculated ratios exhibit similar values in all bands of a given parity, but differ significantly in the transitional nuclei with $A = 151$.

We have shown that the characteristic mean-field and spectroscopic properties of odd-A Eu and Sm nuclei as functions of the neutron number, as well as those of the even-even Sm isotopes, exhibit a rapid change close to the transitional nuclei with mass $A = 151$ or 153. To identify more precisely the location of discontinuities characteristic of
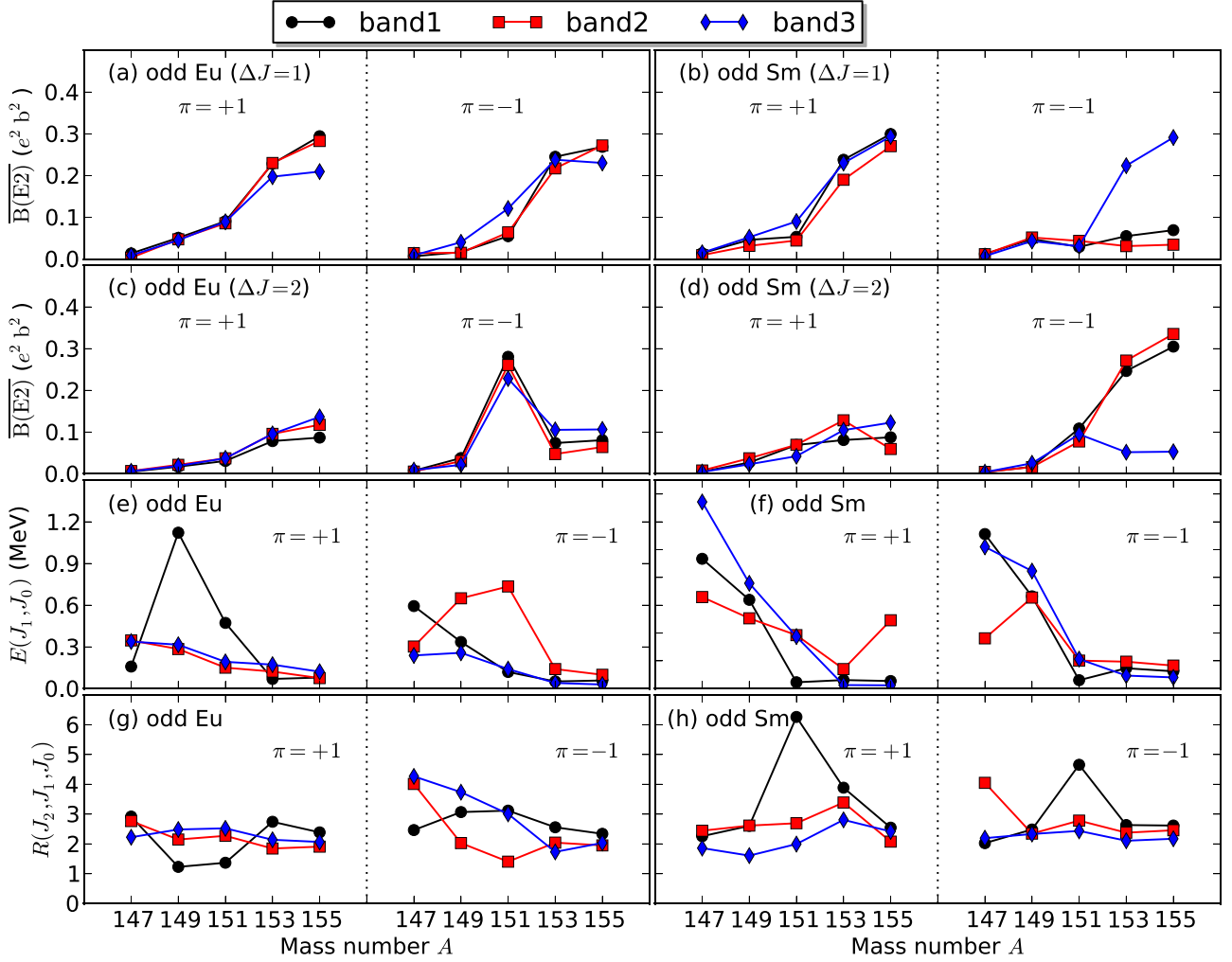
FIG. 10. Dependence on mass number of the calculated spectroscopic quantities for the odd-A Eu and Sm isotopes: average $B(E2; J_0 + \Delta J \rightarrow J_0)$ (in units of $e^2 b^2$) for transitions between the bandhead J_0 of a given band and the lowest five states with $J_0 + \Delta J$, with $\Delta J = 1$ [(a) and (b)] and 2 [(c) and (d)]; the excitation energy $E(J_1, J_0)$ ($J_1 = J_0 + \Delta J$, in MeV) of the second-lowest state in a band relative to the bandhead [(e) and (f)], and the energy ratio $R(J_2, J_1, J_0)$ with $J_2 = J_0 + 2\Delta J$ [(g) and (h)]. See the main text for the definition of each quantity.

shape phase transitions we consider the differentials of these quantities, that is, the difference of their values in neighboring isotopes. The relevance of differential observables for studies of structural evolution of nuclear systems, especially in exotic nuclei, was already pointed out in Ref. [52], where experimental differential observables related to mean-square charge radii, spectroscopic properties, and mass observables of even-even nuclei were analyzed for different regions in the nuclear chart. To facilitate a similar analysis in the case of odd-A nuclei in which the density of low-energy levels is much higher, here we define the differential of a given quantity $\mathcal{O}$ for a nucleus with mass A as its absolute value averaged over the lowest bands i, that is,

$$\delta\mathcal{O} = \frac{1}{n} \sum_{i=1}^{n} |\mathcal{O}_{i,A} - \mathcal{O}_{i,(A-2)}|. \qquad (11)$$

Figure 11 displays the differentials of the mean value $\delta\bar{\beta}$ [panels (a-1) and (a-2)] and variance $\delta\Delta\beta$ [(b-1) and (b-2)]

of the quadrupole deformation β, the q invariants $\delta\overline{B(E2)}$ in the cases of $\Delta J = 1$ [(c-1) and (c-2)] and $\Delta J = 2$ [(d-1) and (d-2)], the energy $\delta E(J_1, J_0)$ [(e-1) and (e-2)], and the ratio $\delta R(J_2, J_1, J_0)$ [(f-1) and (f-2)], averaged over the lowest three ($n = 3$) positive- and negative-parity bands in the odd-A Eu and Sm isotopes. One notices that apart from only a few exceptions, that is, $\delta\overline{B(E2)}$ in the case of $\Delta J = 2$ for the positive-parity states in odd Sm [Fig. 11(d-2)] and $\delta E(J_1, J_0)$ for the positive-parity states in odd Eu [Fig. 11(e-1)], the differentials of the considered quantities exhibit a pronounced discontinuity at the transitional nuclei, where the potential becomes notably soft in both deformation parameters β and γ (cf. Fig. 1): either at $A = 151$ or 153. In Fig. 12 we plot the differentials of the same quantities but for the even-even Sm isotopes. Note that the average in Eq. (11) is taken over the lowest three $K^\pi = 0^+$ bands for $\delta\bar{\beta}$ and $\delta\Delta\beta$, and for the lowest two $K^\pi = 0^+$ bands for $\delta\overline{B(E2)}$, $\delta E(2^+, 0^+)$ and $\delta R(4^+, 2^+, 0^+)$. These plots clearly show that the differentials of the characteristic quantities in the even-even core nuclei also
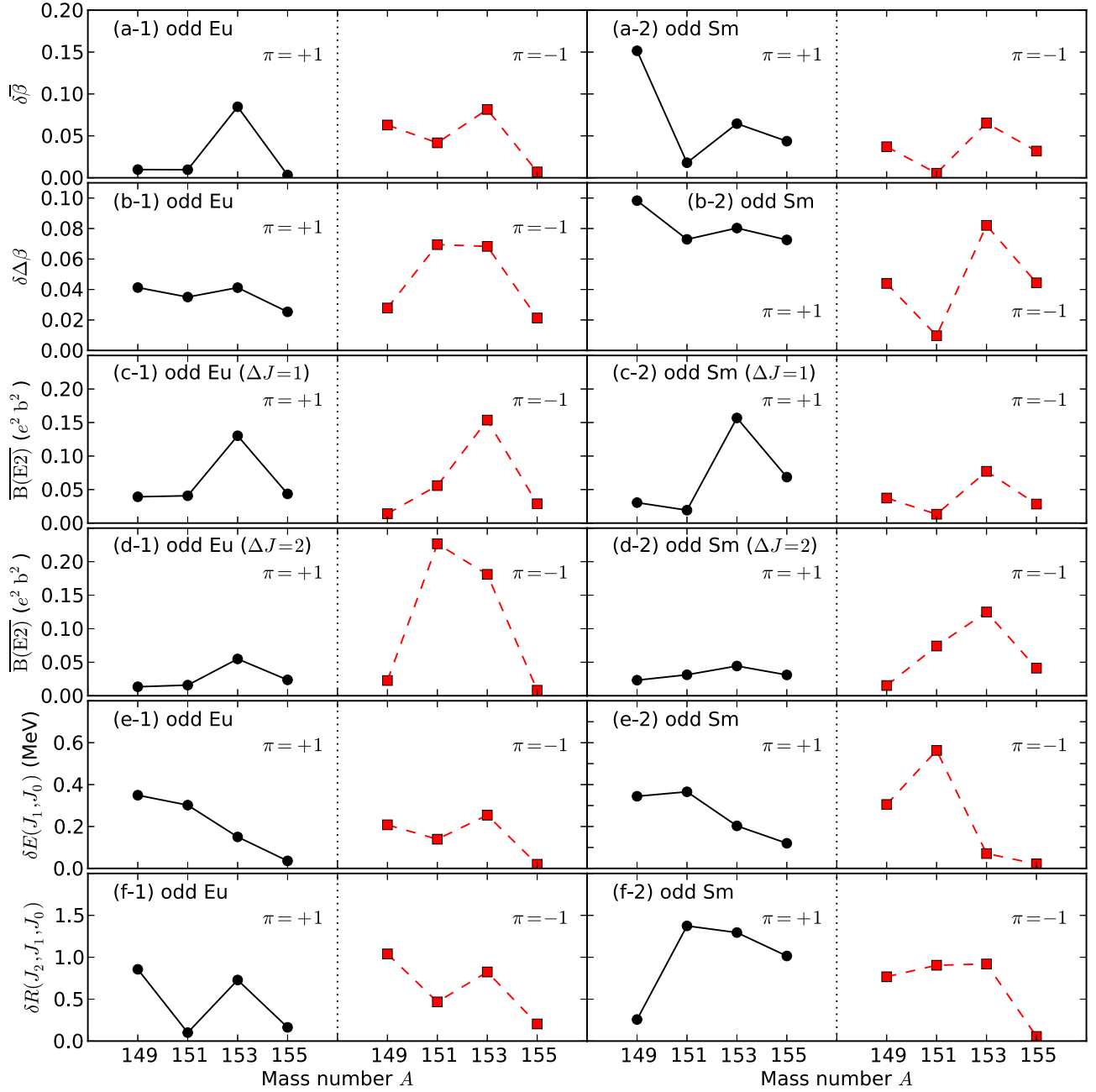
FIG. 11. Differentials of the mean value $\delta\overline{\beta}$ [(a-1) and (a-2)] and variance $\delta\Delta\beta$ [(b-1) and (b-2)] of the quadrupole deformation parameter β, q invariants $\overline{B(E2)}$ with $\Delta J = 1$ [(c-1) and (c-2)], and $\Delta J = 2$ [(d-1) and (d-2)], excitation energy $\delta E(J_1, J_0)$ [(e-1) and (e-2)], and the energy ratio $\delta R(J_2, J_1, J_0)$, for the odd-A Eu and Sm isotopes, as functions of the mass number.

exhibit abrupt changes between the nuclei with mass number $A = 150$ and 152, and these changes correspond to the ones observed in the odd-proton and odd-neutron systems.

Finally, as yet another clear signature of the QPT, we display in Fig. 13 the proton and neutron separation energies [s_p (a) and s_n (b)] and their corresponding differentials [δs_p (c) and δs_n (d)] for the odd-A Eu and Sm isotopes, respectively. The separation energies are obtained simply as the difference between the eigenvalues of the Hamiltonians $\hat{H}$ and $\hat{H}_B$ for the corresponding ground states. Consistent with the results for the other characteristic quantities discussed above, both δs_p and

δs_n exhibit a sharp irregularity at the transitional nuclei with mass number $A = 151$ and 153, for the odd-A Eu and Sm isotopes, respectively.

IV. CONCLUSIONS

A microscopic study of a quantum phase transition related to the shape of odd-mass nuclei has been carried out using a newly developed method of Ref. [20], based on nuclear density functional theory (DFT) and the particle-core coupling scheme. The deformation energy surface for the even-even
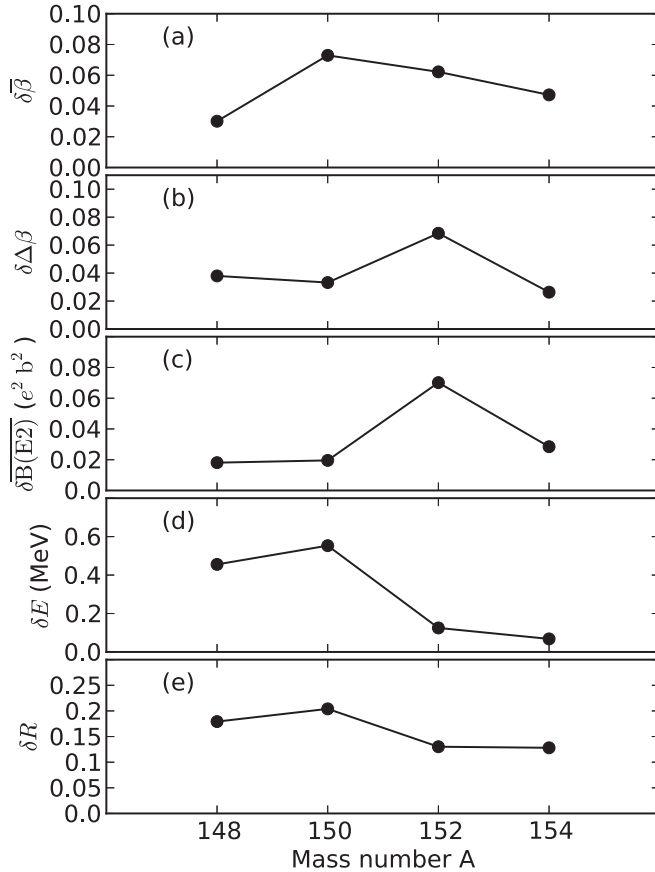
FIG. 12. Same as in the caption to Fig. 11, but for the even-even Sm core nuclei.

FIG. 13. Proton (a) and neutron (b) separation energies (s_p and s_n), and their differentials δs_p (c) and δs_n (d), for the odd-A Eu and Sm isotopes, respectively.

core nuclei, and the single-particle energies and occupation probabilities of the odd fermion (proton or neutron), are obtained from SCMF calculations based on a choice of the energy density functional and pairing interaction. The self-consistent mean-field results determine the parameters of the IBFM Hamiltonian that is used to calculate spectroscopic properties of odd Eu and Sm nuclei with mass number $A = 147$–155. The corresponding even-even core Sm isotopes present one of the best examples of a QPT between spherical and axially deformed shapes. By using this method, characteristic mean-field and spectroscopic properties that can be related to quantum order parameters of the QPT have
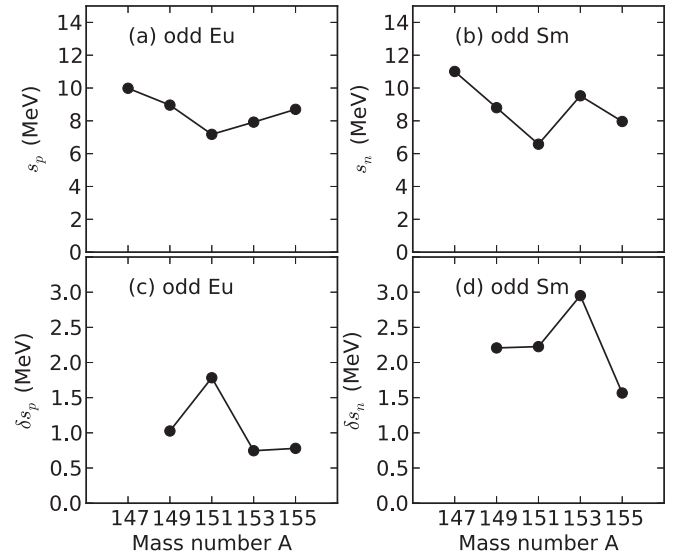
been analyzed and, in particular, the differentials of these quantities that underline the QPT. Even though systems with a finite number of particles have been investigated, and the control parameter is the integer value of the nucleon number rather than a continuous parameter, the differentials of several characteristic quantities (deformation parameter, q invariants, excitation energies, and separation energies) in the odd-A Eu and Sm nuclei, as well as for the even-even Sm cores, all exhibit a clear discontinuity close to $N = 90$ which signals the QPT associated with the softness of the collective potential in transitional nuclei. The results are robust and general, and present a valuable contribution towards a systematic study of shape phase transitions in odd-mass nuclei.

[1] L. Carr (ed.), *Understanding Quantum Phase Transitions* (CRC Press, Boca Raton, FL, 2010).

[2] P. Cejnar, J. Jolie, and R. F. Casten, Rev. Mod. Phys. **82**, 2155 (2010).

[3] A. Bohr and B. M. Mottelsson, *Nuclear Structure*, Vol. 2 (Benjamin, New York, 1975).

[4] R. F. Casten, *Nuclear Structure from a Simple Perspective* (Oxford University Press, Oxford, UK, 1990).

[5] F. Iachello, Rivista del Nuovo Cimento **34**, 617 (2011).

[6] P. Stránský, M. Macek, and P. Cejnar, Ann. Phys. (NY) **345**, 73 (2014).

[7] P. Stránský, M. Macek, A. Leviatan, and P. Cejnar, Ann. Phys. (NY) **356**, 57 (2015).

[8] P. Cejnar, P. Stránský, and M. Kloc, Phys. Scr. **90**, 114015 (2015).

[9] F. Iachello, A. Leviatan, and D. Petrellis, Phys. Lett. B **705**, 379 (2011).

[10] D. Petrellis, A. Leviatan, and F. Iachello, Ann. Phys. (NY) **326**, 926 (2011).

[11] T. Nikšić, D. Vretenar, G. A. Lalazissis, and P. Ring, Phys. Rev. Lett. **99**, 092502 (2007).

[12] L. M. Robledo, R. R. Rodríguez-Guzmán, and P. Sarriguren, Phys. Rev. C **78**, 034314 (2008).

[13] Z. P. Li, T. Nikšić, D. Vretenar, and J. Meng, Phys. Rev. C **80**, 061301 (2009).

[14] K. Nomura, D. Vretenar, and B.-N. Lu, Phys. Rev. C **88**, 021303 (2013).

[15] A. Bohr, Mat. Fys. Medd. Dan. Vid. Selsk. **27**, 16 (1953).

[16] M. Böyükata, C. E. Alonso, J. M. Arias, L. Fortunato, and A. Vitturi, Phys. Rev. C **82**, 014317 (2010).

[17] M. Böyükata, C. E. Alonso, J. M. Arias, L. Fortunato, and A. Vitturi, J. Phys. Conf. Ser. **580**, 012047 (2015).

[18] Y. Zhang, F. Pan, Y.-X. Liu, Y.-A. Luo, and J. P. Draayer, Phys. Rev. C **88**, 014304 (2013).

[19] Y. Zhang, L. Bao, X. Guan, F. Pan, and J. P. Draayer, Phys. Rev. C **88**, 064305 (2013).

[20] K. Nomura, T. Nikšić, and D. Vretenar, Phys. Rev. C **93**, 054305 (2016).

[21] M. Bender, P.-H. Heenen, and P.-G. Reinhard, Rev. Mod. Phys. **75**, 121 (2003).

[22] D. Vretenar, A. Afanasjev, G. Lalazissis, and P. Ring, Phys. Rep. **409**, 101 (2005).

[23] T. Nikšić, D. Vretenar, and P. Ring, Prog. Part. Nucl. Phys. **66**, 519 (2011).

[24] F. Iachello and A. Arima, *The Interacting Boson Model* (Cambridge University Press, Cambridge, UK, 1987).

[25] F. Iachello and P. Van Isacker, *The Interacting Boson-Fermion Model* (Cambridge University Press, Cambridge, UK, 1991).

[26] F. Iachello, Phys. Rev. Lett. **87**, 052502 (2001).

[27] T. Otsuka, A. Arima, and F. Iachello, Nucl. Phys. A **309**, 1 (1978).

[28] *Interacting Bose-Fermi Systems in Nuclei*, edited by F. Iachello (Springer, New York, 1981).

[29] O. Scholten, Prog. Part. Nucl. Phys. **14**, 189 (1985).

[30] K. Nomura, N. Shimizu, and T. Otsuka, Phys. Rev. Lett. **101**, 142501 (2008).

[31] J. N. Ginocchio and M. W. Kirson, Nucl. Phys. A **350**, 31 (1980).

[32] T. Otsuka and N. Yoshida, JAERI-M (Japan Atomic Energy Research Institute) Report No. 85, 1985.

[33] R. F. Casten, M. Wilhelm, E. Radermacher, N. V. Zamfir, and P. von Brentano, Phys. Rev. C **57**, R1553 (1998).

[34] N. V. Zamfir, R. F. Casten, M. A. Caprio, C. W. Beausang, R. Krücken, J. R. Novak, J. R. Cooper, G. Cata-Danil, and C. J. Barton, Phys. Rev. C **60**, 054312 (1999).

[35] T. Klug, A. Dewald, V. Werner, P. von Brentano, and R. Casten, Phys. Lett. B **495**, 55 (2000).

[36] R. Krücken, B. Albanna, C. Bialik, R. F. Casten, J. R. Cooper, A. Dewald, N. V. Zamfir, C. J. Barton, C. W. Beausang, M. A. Caprio *et al.*, Phys. Rev. Lett. **88**, 232501 (2002).

[37] D. Tonev, A. Dewald, T. Klug, P. Petkov, J. Jolie, A. Fitzler, O. Möller, S. Heinze, P. von Brentano, and R. F. Casten, Phys. Rev. C **69**, 034334 (2004).

[38] O. Möller, A. Dewald, P. Petkov, B. Saha, A. Fitzler, K. Jessen, D. Tonev, T. Klug, S. Heinze, J. Jolie *et al.*, Phys. Rev. C **74**, 024313 (2006).

[39] W. D. Kulp, J. L. Wood, P. E. Garrett, C. Y. Wu, D. Cline, J. M. Allmond, D. Bandyopadhyay, D. Dashdorj, S. N. Choudry, A. B. Hayes *et al.*, Phys. Rev. C **77**, 061301 (2008).

[40] R. F. Casten and N. V. Zamfir, Phys. Rev. Lett. **87**, 052503 (2001).

[41] E. A. McCutchan, N. V. Zamfir, and R. F. Casten, Phys. Rev. C **69**, 064306 (2004).

[42] E. A. McCutchan, N. V. Zamfir, and R. F. Casten, Phys. Rev. C **71**, 034309 (2005).

[43] V. Werner, E. Williams, R. J. Casperson, R. F. Casten, C. Scholl, and P. von Brentano, Phys. Rev. C **78**, 051303 (2008).

[44] Z. P. Li, T. Nikšić, D. Vretenar, J. Meng, G. A. Lalazissis, and P. Ring, Phys. Rev. C **79**, 054301 (2009).

[45] T. Nikšić, D. Vretenar, and P. Ring, Phys. Rev. C **78**, 034318 (2008).

[46] Y. Tian, Z. Y. Ma, and P. Ring, Phys. Lett. B **676**, 44 (2009).

[47] Brookhaven National Nuclear Data Center, http://www.nndc.bnl.gov

[48] V. Paar, S. Brant, L. Canto, G. Leander, and M. Vouk, Nucl. Phys. A **378**, 41 (1982).

[49] A. Leviatan, Phys. Lett. B **209**, 415 (1988).

[50] K. Kumar, Phys. Rev. Lett. **28**, 249 (1972).

[51] D. Cline, Annu. Rev. Nucl. Part. Sci. **36**, 683 (1986).

[52] R. B. Cakirli, R. F. Casten, and K. Blaum, Phys. Rev. C **82**, 061306 (2010).